

The Extreme Ultraviolet Deficit and Magnetically Arrested Accretion in Radio Loud Quasars

Brian Punsly¹

ABSTRACT

The Hubble Space Telescope composite quasar spectra presented in Telfer et al. show a significant deficit of emission in the extreme ultraviolet (EUV) for the radio loud component of the quasar population (RLQs), compared to the radio quiet component of the quasar population (RQQs). The composite quasar continuum emission between 1100 Å and ~ 580 Å is generally considered to be associated with the innermost regions of the accretion flow onto the central black hole. The deficit between 1100 Å and 580 Å in RLQs has a straightforward interpretation as a missing or a suppressed innermost region of local energy dissipation in the accretion flow. It is proposed that this can be the result of islands of large scale magnetic flux in RLQs that are located close to the central black hole that remove energy from the accretion flow as Poynting flux (sometimes called magnetically arrested accretion). These magnetic islands are natural sites for launching relativistic jets. Based on the Telfer et al. data and the numerical simulations of accretion flows in Penna et al., the magnetic islands are concentrated between the event horizon and an outer boundary of $< 2.8M$ (in geometrized units) for rapidly rotating black holes and $< 5.5M$ for modestly rotating black holes.

Subject headings: Black hole physics — magnetohydrodynamics (MHD) — galaxies: jets—galaxies: active — accretion, accretion disks

1. Introduction

The nature of the causative agent that makes some quasars radio loud (RLQs) has challenged astrophysicists for more than 50 years. It became clear early on that the optical/ultraviolet (UV) spectra of RLQs and radio quiet quasars (RQs) are very similar

¹1415 Granvia Altamira, Palos Verdes Estates CA, USA 90274 and ICRANet, Piazza della Repubblica 10 Pescara 65100, Italy, brian.punsly1@verizon.net or brian.punsly@comdev-usa.com

(Steidel and Sargent 1991)¹. Attempts to look for subtle differences involved statistical studies of optical and UV emission line strengths and widths (Boroson and Green 1992; Boroson 2002; Corbin and Francis 1994; Corbin and Boroson 1996; Brotherton et al 1994). These emission regions are far from the central engine, $\sim 10^3 - 10^4$ larger than the central black hole radius, so it is not clear what they tell us as a second order indicator of conditions in the jet launching region (Guerras et al. 2013). Are they related to the fueling mechanism for radio loudness, the ionization continuum or jet propagation? Consequently, this research path has provided very little understanding of the jet launching mechanism. Seemingly more relevant to the physics of jet launching, the extreme ultraviolet (EUV) continuum, $\lambda < 1100 \text{ \AA}$, is created orders of magnitude closer to the central engine and RLQs display a significant EUV continuum deficit relative to RQs (Telfer et al. 2002), **T02** hereafter.

In the following, evidence is presented that connects the EUV deficit to magnetically arrested accretion (MAA) in the innermost accretion flow of RLQs. The motivation for exploring this interpretation is that it not only explains the second order effect of an EUV deficit, but it also provides a mechanism for the first order difference between RLQs and RQs; namely arresting the flow with large scale magnetic flux is a natural way to launch the jets responsible for the radio emission. This argument is laid out as follows. Section 2 considers the EUV emission in the context in the standard interpretation of a quasar as emission from an optically thick thermal gas that accretes onto a black hole. Section 3 reviews the notion of MAA. Based on the assumption that the EUV deficit is a consequence of thermal gas being displaced by islands of large scale magnetic flux, the distribution of said islands is determined from both numerical and theoretical models of accretion flows.

2. The Thermal Interpretation of Quasar Spectra

It was convincingly demonstrated in Lynden-Bell and Rees (1971); Shakura and Sunayev (1973); Novikov and Thorne (1973) that the intense blue/UV light associated with the quasar phenomenon was likely the optically thick thermal emission from viscous dissipation of accreting gas onto a supermassive black hole. The connection between these accretion models and observation was made in Malkan (1983); Szuszkiewicz et al. (1996) where quasar spectra in the the optical to far UV were approximated by accretion disks spectra. Our understand-

¹There are notable small subclasses of objects that are distinct. Some RLQs have relativistic jets that propagate close to the line of sight (blazars) and the Doppler enhanced power law continuum can be significant. There are also rare objects with very broad ultraviolet absorption lines, these are almost exclusively RQs. However, in both classes these effects obfuscate a background thermal component that is very similar to other quasars.

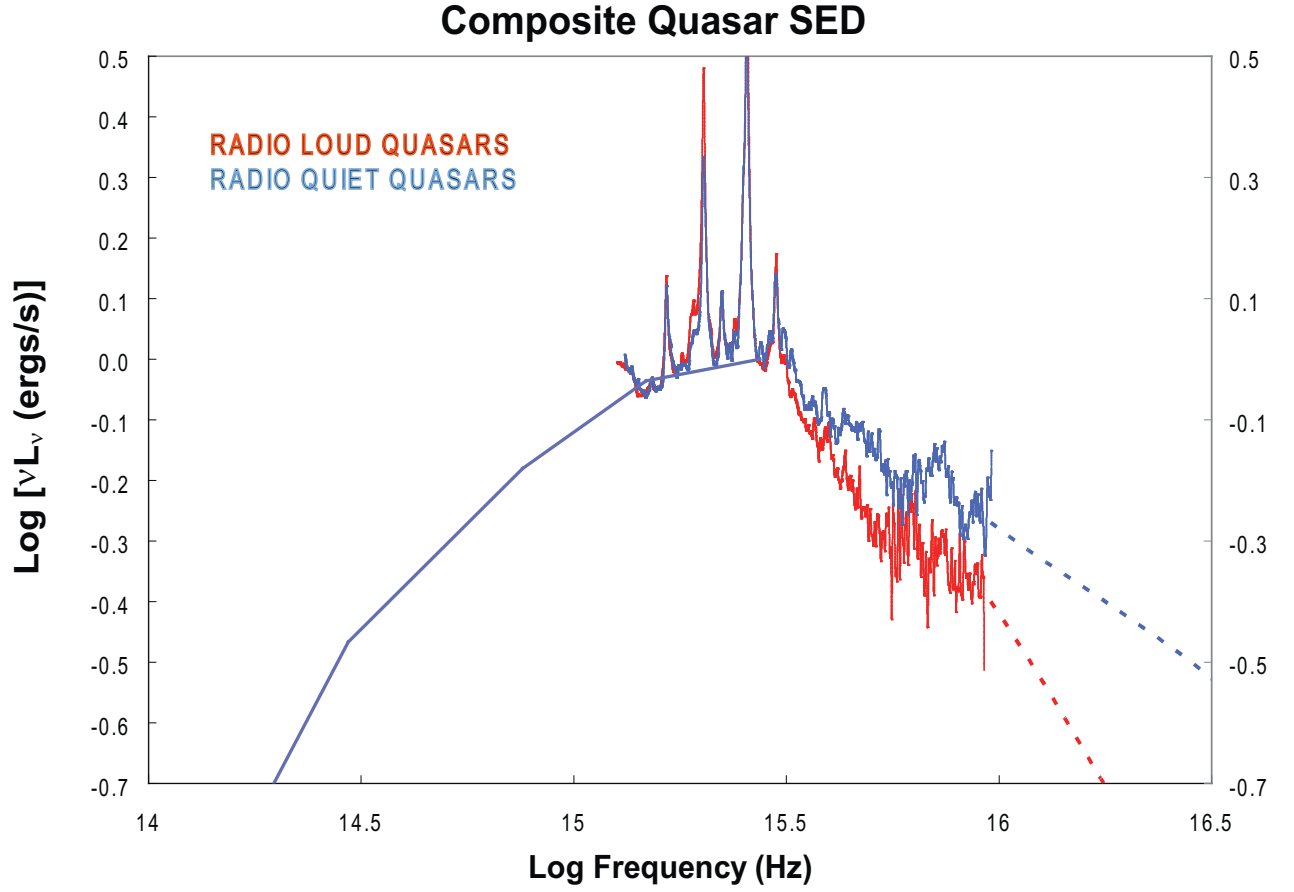


Fig. 1.— The quasar composite continuum accretion disk SED. The black lines represent the common UV/optical/IR continuum. The blue and red plots are the EUV composite spectra for RQs and RLQs from **T02**, respectively.

ing of accretion disks around black holes is far from complete. Thus, this effort strives to reach conclusions that do not depend on a particular accretion model. Determination of the EUV spectrum beyond the far UV turnover had to await space-based observations of intermediate redshift quasars since ground-based observations of high redshift objects, in which the EUV is redshifted into the optical band, are unsuitable due to contamination by the Ly α forest (Zheng et al. 1997).

The EUV deficit in RLQs was originally found in Zheng et al. (1997) and confirmed with a much larger sample of spectra in **T02**. Figure 1 shows the composite RLQ (red) and RQ (blue) EUV spectra, 1100 Å to 300 Å, from Hubble Space Telescope (HST) observations of 332 spectra of 184 objects with redshift, $z > 0.33$ **T02**². The quasar accretion disk composite in Figure 1 is based on the Laor et al. (1997) composite, but it is updated with the optical and IR composite quasar estimates in Davis and Laor (2011). They note the important point that the IR (dust) local maximum should be neglected in estimates of the accretion flow SED because it is likely to be the result of accretion disk emission that is reprocessed on larger scales. The UV composite is updated based on the data and discussion in **T02**. The small difference in the UV continuum between the RLQ and RQ composites in Laor et al. (1997) does not exist (see Figure 10 of **T02**) in the larger HST sample. The common continuum at frequencies below the far UV for the accretion disk composite of RQs and RLQs is represented by a black piecewise power-law fit. The EUV is the data of interest, so it is plotted explicitly as opposed to the piecewise power-law estimates elsewhere. The EUV data is normalized to 0 at 1100 Å as in **T02**. The SEDs above 6×10^{15} Hz show a spectral break, but they are very noisy and are not considered reliable in this region. At frequencies above 10^{16} Hz, where the **T02** data ends, the SED is very uncertain and is indicated by faint dotted lines. These extend to the soft X-ray values (relative to the peak of the SED) from Laor et al. (1997). Since the X-ray luminosity is not considered optically thick thermal emission from the accretion flow and its value relative to the EUV is quite uncertain, it will not be plotted or considered in detail in the following.

It should be noted that both numerical and analytic models of optically thick accretion flows contain the following elements: the effective temperature increases as the radius decreases and the luminosity from each annular ring reaches a maxima near the black hole and decreases inward of this, i.e., the luminosity of the accreting gas fades before being

²The newer HST spectra in Stevans et al. (2014) have a span $< 1/2$ of the G160L spectra (that was commonly used in **T02** to bridge the far UV and EUV) and are not wide enough to use in Figure 2. The small number (8) of narrow span RLQ spectra entirely within the EUV, above the noisy spectral break at $\approx 550\text{Å}$ of Figure 1 ($1100\text{Å} < \lambda < 550\text{Å}$), render statistical comparison to RQs insignificant. The FUSE composite in Scott et al. (20004) has only two RLQs with coverage below 700 Å.

swallowed by the black hole (Zhu et al. 2012). Thus, we expect that the maximum of the SED is not representative of the maximum temperature of the accretion flow, but there are higher temperature contributions to the SED beyond the far UV turnover from optically thick thermal gas. Thus, the rapidly falling SED in the EUV band is the electromagnetic signal of the innermost optically thick region. Consider this in the context of the broadband composite of Figure 1. The continuum of the thermal component (frequencies below 6×10^{15} Hz) of RLQs and RQs are indistinguishable except for emission from the innermost accreting optically thick gas. Thus, the difference in the EUV emission between RLQs and RQs likely arises from suppressed emission in the innermost region of the accretion flow in RLQs of what is otherwise a similar accretion flow to that found in RQs.

3. The EUV Deficit and Magnetically Arrested Accretion

The viscous dissipation that heats the plasma in accretion flows (and therefore the source of modified black body radiation) is produced as a consequence of the magneto-rotational instability (MRI) in 3-D numerical simulations (Penna et al 2010; De Villiers et al. 2003). The discussion of the last section begs the question, what physical process in the innermost accretion flow can suppress MRI in RLQs? The answer might be MAA, Igumenshchev et al (2003); Igumenshchev (2008), or its variants MCAFs (magnetically choked accretion flows), McKinney et al (2012) and MADs (magnetically arrested disks), Tchekhovskoy et al. (2011, 2012). The accretion flow in these simulations is perforated by large scale magnetic flux tubes, magnetic islands. The islands of magnetic flux that arrest the accretion flow also suppress the MRI induced dissipation in these regions. The magnetic flux tubes torque the plasma and enhance the overall mass accretion rate. The angular momentum is converted to electromagnetic form and removed vertically from the accretion flow as a jet (Igumenshchev 2008). Without loss of generality, consider an annular ring in the Shakura and Sunayev (1973) accretion disk, $r_1 < r < r_2$. Angular momentum is removed by viscous stress in the fluid element at a rate

$$T_{\phi;\nu}^{\nu} = 0 \implies \dot{L} = \dot{m}(\Omega(r_2)r_2^2 - \Omega(r_1)r_1^2) = \int r^{-2}(r^2 T_{\phi}^r{}^{\text{visc}})_{,r} dV, \quad (1)$$

where $T_{r\phi}^{\text{visc}}$ is the viscous stress, \dot{m} is the accretion rate and $\Omega(r)$ is the angular velocity. Now consider the existence of magnetic islands that fill a fraction, f_V , of the volume of the ring, V , and penetrate a fraction, f , of the top and bottom surface areas of the annular volume, SA . The volume of magnetic islands is V_{MI} and its complement in V is V_{MI}^C , $f_V = \int dV_{MI}/V$. The surface area elements of the top and bottom faces are, dSA_{MI} and dSA_{MI}^C , respectively.

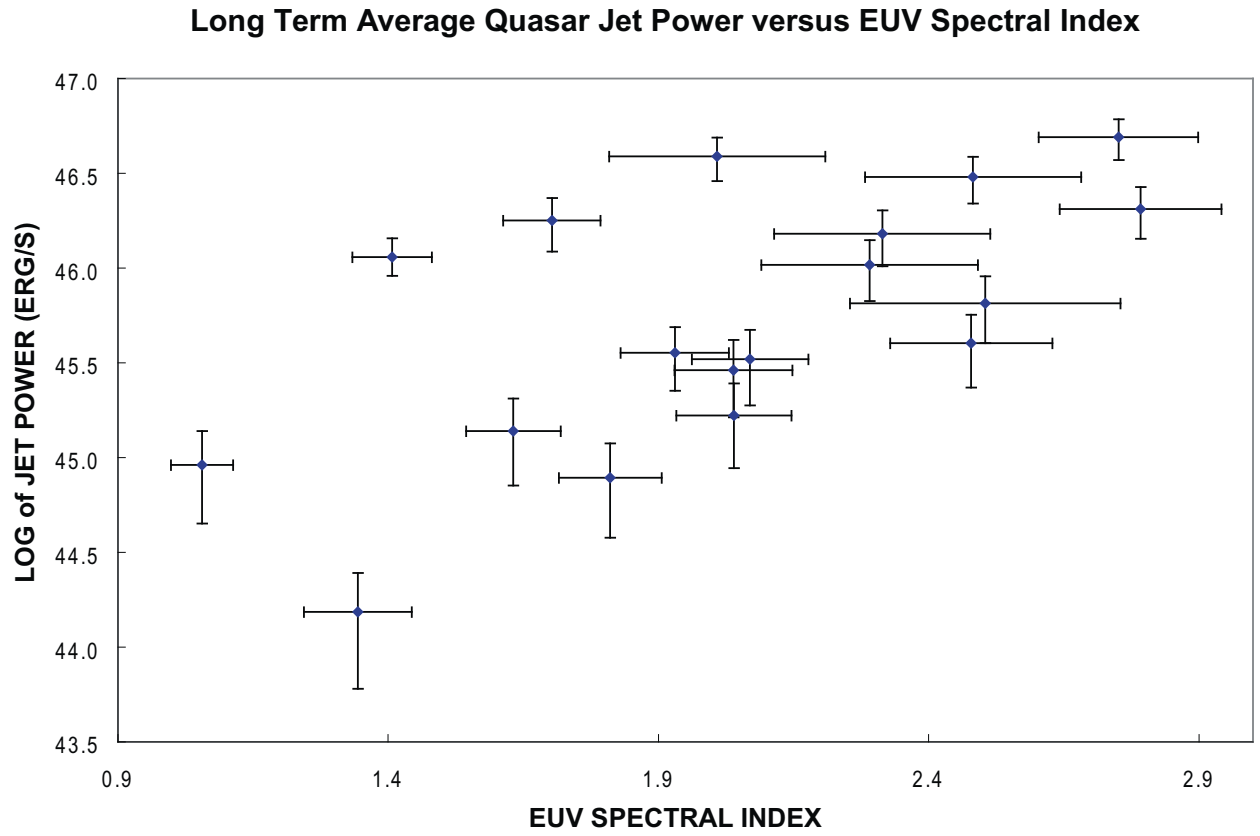


Fig. 2.— A scatter plot of the estimated jet power and the EUV spectral index in frequency space (a value of 1 is a flat SED).

The angular momentum equation becomes

$$\dot{L} = \dot{m}(\Omega(r_2)r_2^2 - \Omega(r_1)r_1^2) = \int r^{-2}(r^2 T_{\phi}^r)^{\text{visc}}{}_{,r} dV_{MI}^C + \int (-r B^{\phi} B^z / (8\pi))_{,z} dV_{MI}, \quad (2)$$

where, B^{ϕ} and B^z are the azimuthal and vertical magnetic field components, respectively. For \dot{m} fixed in Equations (2) and (3), even though the volume of plasma experiencing viscous dissipation is reduced, accretion proceeds at an equal rate in the magnetically arrested state.

Simulated MAD accretion flows are subsonic and therefore do not produce significant gas heating from shocks (McKinney et al 2012; Punsly and Rodriguez 2013). Thus, the reconnection of the locally tangled field driven by the MRI is the primary source of heat creation at the boundary of the magnetic islands and in the accreting gas. However, the interior of the magnetic islands are not regions of local MRI driven heating. The total volume available for MRI induced viscous heating is reduced by the magnetic islands. Therefore, the MRI suppression in magnetically arrested flows indicate states of lower radiative efficiency relative to standard accretion states without magnetic islands. The magnetic islands radiate Poynting flux along the magnetic field lines. Again consider the annular ring above. The total energy flux, $Q = Q^{\text{visc}} + Q^{\text{jet}}$, has two components, where Q^{visc} is the flux of radiation as in a standard accretion disk and Q^{jet} is primarily poloidal Poynting flux along the magnetic field direction, S^P (Igumenshchev 2008). Similarly, the total luminosity P of the ring also has two components:

$$P = \int Q dA = (1/2) \int r(d\Omega/dr) T_{r\phi}^{\text{visc}} dz dSA_{MI}^C + \int S^P dSA_{MI}. \quad (3)$$

The first term on the RHS of Equation (3) is the usual term from standard accretion theory that gives rise to the radiation (such as EUV). The second term is the vertical jet emission. For any approximately axisymmetric MHD Poynting flux dominated jet, regardless of the source, the total integrated electromagnetic poloidal energy flux is

$$\int S^P dA_{\perp} = (\Omega_F/c) \int (-r B^{\phi} B^z / (8\pi))_{,z} dV_{MI} \approx k \frac{\Omega_F^2 \Phi^2}{2\pi^2 c}, \quad (4)$$

where Φ is the total magnetic flux enclosed within the jet, dA_{\perp} is the cross-sectional area element and k is a geometrical factor that equals 1 for a uniform highly collimated jet (Punsly 2008). Thus, not only do the magnetic islands of large scale poloidal flux in the inner accretion flow suppress radiation from this region, but they provide a source of Poynting flux (power for the jet) as they orbit around the black hole with an angular velocity, Ω_F . The local physics that produces the turbulent viscosity, η_t , in V_{MI}^C is unchanged from standard accretion and therefore so is $T_{r\phi}^{\text{visc}} = \eta_t r(d\Omega/dr)$. Thus, from Equations (1) - (4), in the

magnetically arrested case, the radiative luminosity is $\approx 1 - f$ of what it would be for standard accretion with the same mass accretion rate.

If MAA is the source of the EUV deficit, one would expect a correlation (perhaps weak) between the EUV spectral index, α_{EUV} , and jet power within the RLQ population. In Figure 2, α_{EUV} ($F_\nu \sim \nu^{-\alpha_{\text{EUV}}}$) derived from individual spectra in the HST archives (downloaded through MAST) is plotted against estimates of the long term time average of the jet power, \overline{Q} . In order to get a meaningful estimate of α_{EUV} , a range of at least 700 Å to 1100 Å in the quasar rest frame was needed to extract the continuum from the numerous broad emission lines documented in **T02**. Therefore, a redshift of $z > 0.63$ is required. Troughs from Lyman limit systems (LLS) were removed by assuming a single cloud with a ν^{-3} opacity. This was considered acceptable if the power law above the LLS could be continued smoothly through the corrected region. If there were many strong absorption systems or an LLS that compromised a broad emission line, this simple procedure was deemed inadequate for continuum extraction with the available data and the spectrum was eliminated from the sample. A small correction for the Lyman valley was also made per the methods of Zheng et al. (1997). Additionally, if there was evidence of a blazar synchrotron component contribution to the continuum (high optical polarization or variability, superluminal motion or gamma ray activity), the underlying accretion disk continuum was considered too uncertain for the sample.

The most reliable methods of estimating \overline{Q} are based on the the optically thin emission from relaxed radio lobes (Willott et al. 1999). Thus, all sources in the sample needed proof of extended emission on scales larger than the host galaxy so that the lobes can relax (> 20 kpc). The proof was derived from archival high resolution interferometry images made between 0.408 GHz and 5 GHz. The HST and radio selection criteria resulted in a total of 18 sources for the sample. The optically thin emission was estimated based on 151 MHz - 178 MHz flux densities (if available) and the lobe fluxes from the radio images. The largest spread in the estimates of \overline{Q} , based on optically thin extended emission, are bounded on the high side by the Willott et al. (1999) estimate for their parameter, $\mathbf{f} = 20$, and on the low side by Punsly (2005), which assumes that the lobes are inertially dominated. These two extremes are used to generate the errors bars on \overline{Q} in Figure 2 (Punsly and Rodriguez 2013). The correlation in the scatter in Figure 2 is statistically significant at the 0.987 level by a Spearman rank correlation test, while the correlations of α_{EUV} with z and spectral luminosity, $\lambda L_\lambda(1100\text{\AA})$, are significant at the 0.842 and 0.720 levels, respectively for the same sample. The large scatter in Figure 2 is expected on many grounds: the ejections producing \overline{Q} are not contemporaneous with the the HST spectrum, as well as variations in the quasar host EUV absorption, \dot{m} , black hole masses, (M), and spins (a/M).

Since a magnetically arrested innermost accretion flow naturally explains the suppressed EUV and jet production, it is of interest to estimate the size of the region of suppressed radiation. From the composites in Figure 1, the EUV deficit in RLQs is $\approx 0.045L_{\text{bol}}$ of the optically thick accretion flow³. Consider excising a fraction, f , of the innermost accretion flow in various models of accretion disks in Figure 3. The simulations of accretion disks in Penna et al (2010) include luminosity from the plunge region inside of the innermost stable orbit (ISCO) and are parameterized by a/M and the disk thickness defined by their parameter, h/r . The Novikov and Thorne (1973), NT, models do not include a plunge region. Note that the putative magnetically arrested region must be concentrated at the smallest radii, since the EUV is suppressed in RLQ composite of Figure 1, but not the UV and optical. The plausible range of, $0.3 < f < 0.9$, near the black hole is based on the simulations presented in Igumenshchev (2008); Punsly et al (2009). The putative magnetic islands would have to be concentrated between the event horizon and an outer boundary of $< 2.8M$ if $a/M = 0.98$ and $< 5.5M$ if $a/M = 0.7$ to account for the 4.5% luminosity suppression in RLQs.

It should be noted that, unlike the simulations in Igumenshchev (2008); Punsly et al (2009), the simulations in McKinney et al (2012); Tchekhovskoy et al. (2011, 2012) that are heavily seeded with large scale magnetic flux are devoid of magnetic islands this close to the event horizon. This is evidenced by the claim in McKinney et al (2012) that no significant Poynting flux emerges from this region (see Equation 4, above) as well as the linked online videos of the simulations. The videos show the innermost significant magnetic island concentrations are around $\sim 20M$ and they are extremely transient. This either means that the interpretation of the EUV deficit presented here is wrong or the simulations do not represent the magnetic flux evolution accurately. Using fusion and solar physics as a guide, the latter seems quite likely since these simulations are based on simple single fluid ideal MHD (Yamada 2007; Malakit 2009; Bauman et al 2013; Threlfall et al. 2012). Even more important, the two most relevant dynamic elements for large scale, poloidal, magnetic flux evolution near the black hole, reconnection and diffusion of mass onto the field lines, occur as a consequence of numerical diffusion in the simulations and not an actual physical process.

³The emission line contribution to L_{bol} is chosen to be 25% of the optical/UV luminosity (Zheng et al. 1997). The X-ray contribution to L_{bol} is ignored as discussed in Section 2. Ignoring the X-ray luminosity of the accretion flow proper will affect the estimates by $< 10\%$ (Laor et al. 1997; Davis and Laor 2011).

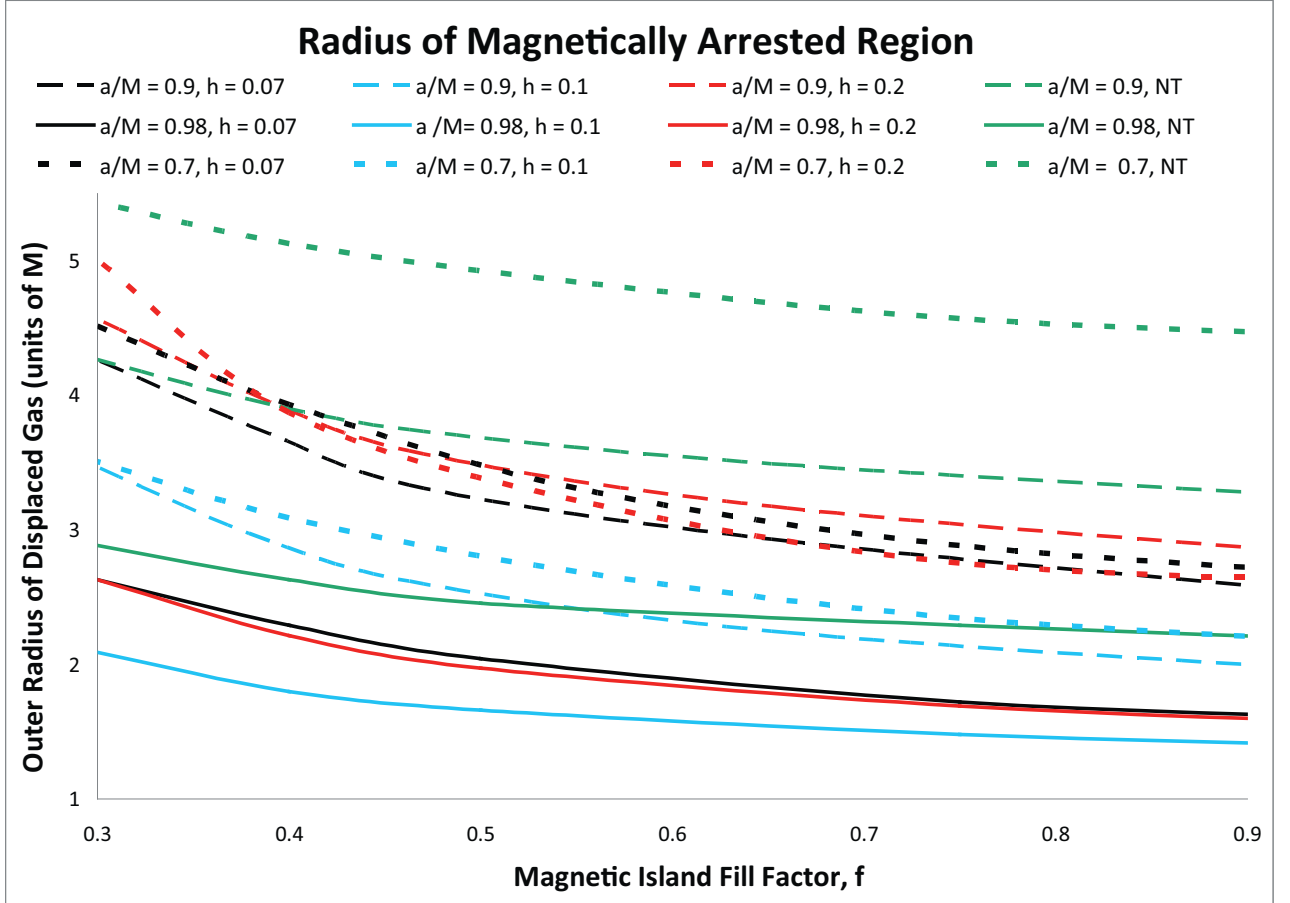


Fig. 3.— The size of the magnetically arrested region required for the EUV deficit in RLQs versus the filling factor for magnetic flux, f , for various models from Penna et al (2010).

4. Discussion

In this paper, the EUV deficit in RLQ SEDs was argued to arise from a deficit of optically thick thermal gas in the innermost accretion flow. It was posited that islands of large scale magnetic flux near the black hole, like those that occur in some numerical simulations, would explain this missing volume of optically thick thermal gas and also explain the radio jet launching mechanism. As a further consequence it was argued in Punsly (1999) that the presence of magnetic flux in the inner accretion disk will diminish the power of radiation driven winds that appear to be common in RQs. It is not claimed that this is the only explanation of the EUV deficit. However, none of the alternatives naturally produce a radio jet. Other explanations based on numerical and theoretical models include, lower a/M in RLQs (larger ISCO), a stronger quenching wind in RLQs per the model of Laor and Davis (2014) or higher M and lower \dot{m} in RLQs. Using a sample of > 6000 QSOs McLure and Jarvis (2004) found that the mean M of RLQs is 1.45 that of of RQs with large scatter. In disk models, larger M shifts the peak of the SED to lower frequency, therefore causing a decrease in the EUV. However, it was shown in Davis and Laor (2011); Laor and Davis (2014), based on PG quasars, that black hole mass variations produce much smaller changes in the far UV turnover region of the spectrum than expected from accretion disk models. Thus the issue needs to be addressed empirically. In Figure 4, the **T02** composites are overlayed. The location of the SED peak and the curvature of the continuum long-ward of the peak are indistinguishable contrary to the notion that a disk temperature shift results in the EUV deficit. Furthermore, if the mass difference is the source of the EUV deficit, the correlation in Figure 2 would be a coincidence.

The basic idea presented here does not depend on any particular accretion model. The observational data indicates that the only significant difference in the optically thick thermal continuum between the RQ and RLQ composite spectra is a deficit of the highest temperature gas (the EUV) in RLQs. This must be created by the innermost optically thick gas independent of the model. A plausible explanation is the displacement of this gas by the large scale magnetic flux of the radio jet at its launch site.

This work benefitted greatly from the input of a very knowledgeable referee who directed the effort towards many important topics that were initially overlooked. I am also indebted to Michael Brotherton who computed the RLQ and RQQ black hole masses from SDSS DR7, for $0.9 < z < 1.1$. Although not directly used due to space constraints, this provided valuable insight. I am also thankful to Robert Antonucci for helping me correct for the Lyman limit systems in the HST spectra. I am extremely grateful to Matt Malkan who reviewed the logic of the arguments presented and implied by the paper with me and also had great insight

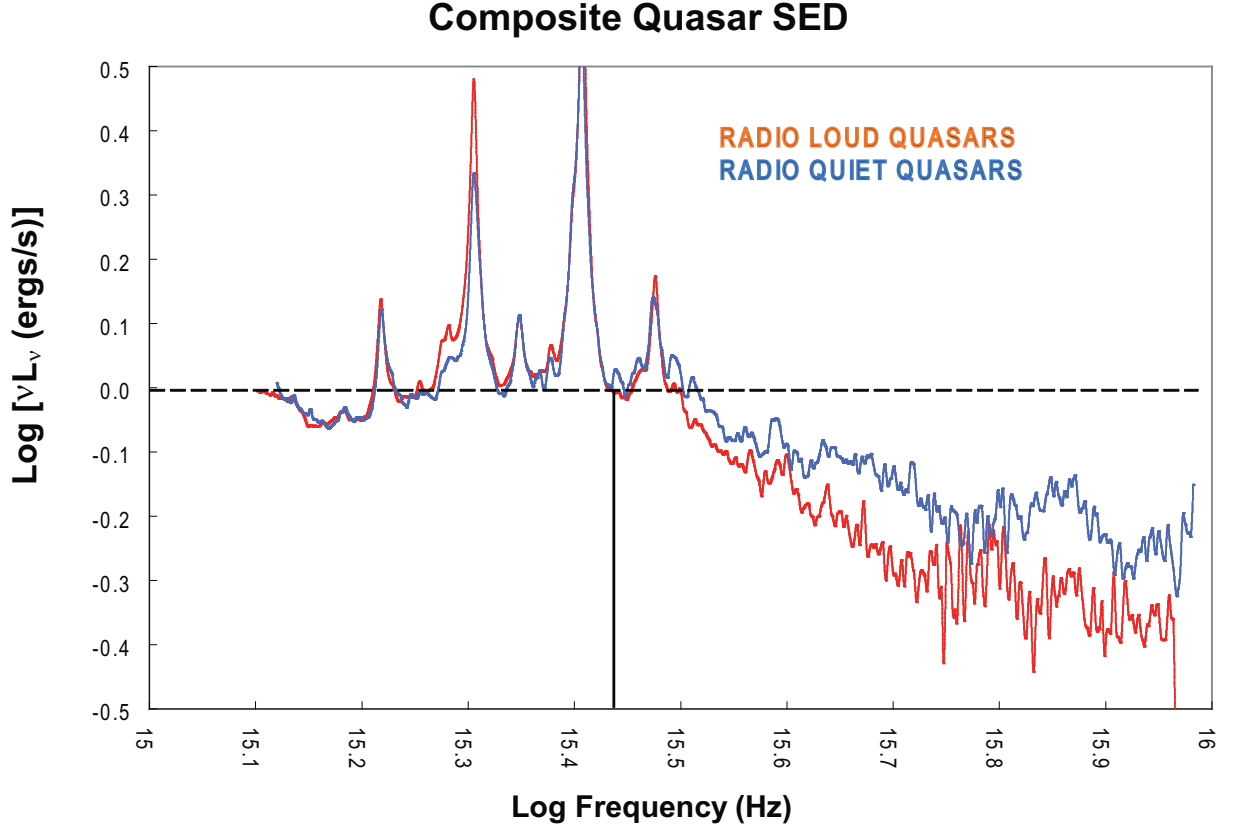


Fig. 4.— The blue and red plots are the composite spectra for RQs and RLQs from **T02**, respectively. The spectral peak and the curvature of the continuum long-ward of the peak are virtually identical. The composites are normalized to 0 at 1100Å. That is indicated by the black lines.

into the proper interpretation of the HST data.

REFERENCES

- Baumann, G., Galsgaard, K. & Norlund, A., 2013 *Solar Physics* 284 467
- Boroson, T. and Green, R. 1992, *ApJS* 80 109
- Boroson, T. 2002, *ApJ* 565 78
- Brotherton, M., Wills, B. Steidel, C. and Sargent, W. 1994, *ApJ* 423 131
- Corbin, M. and Francis, P. 1994, *AJ* 108 2016
- Corbin, M. and Boroson, T. 1996, *ApJS* 107 69
- Czerny, B. and Elvis, M. 1987, *ApJ* 321 305
- Davis, S., Laor, A. 2011, *ApJ* 728 98
- De Villiers, J-P., Hawley, J., Krolik, 2003, *ApJ* 599 1238
- Guerras, E. et al. 2013, *ApJ* 764 160
- Igumenshchev, I. V. 2008, *ApJ* 677 317
- Igumenshchev, I. V., Narayan, R. and Abramowicz, M. A. 2003, *ApJ* 592 1042
- Laor, A. et al 1997, *ApJ* 477 93
- Laor, A., Davis, S. 2014, *ApJ* 428 3024
- Lynden-Bell, D., Rees, M. 1971, *MNRAS* 152 461
- Malakit, K., Cassak, P., Shav, M., Drake, F. 2009, *Geophysical Research Letter* 36 L07107
- Malkan, M. 1983, *ApJ* 268, 582
- McLure, R. and Jarvis, M. 2004, *MNRAS* 353, L45
- McKinney, J., Tchekhovskoy, A., Blandford, R. 2012, *MNRAS* 423 3083
- Novikov, I. and Thorne, K. 1973, in *Black Holes: Les Astres Occlus*, eds. C. de Witt and B. de Witt (Gordon and Breach, New York), 344

- Penna, R. et al 2010, MNRAS 408 752
- Punsly, B. 1999, ApJ 527 609
- Punsly, B. 2005, ApJL 623 9
- Punsly, B. 2008, *Black Hole Gravitohydromagnetics*, second edition (Springer-Verlag, New York)
- Punsly, B., Igumenshchev, I. V., Hirose, S. 2009, ApJ 704, 1065
- Punsly, B., Rodriguez J. 2014, ApJ 783, 113
- Scott, J. et al. 2004, ApJ 615, 135
- Shakura, N., Sunayev, R. 1973, A& A 24 337
- Steidel, C. and Sargent, W., 1991 ApJ 383 433
- Stevens, M., Shull, M., Danforth, C., Tilton, E. 2014, ApJ 794 75
- Szuskiewicz, E., Malkan, A., and Abramowicz, M. A. 1996, ApJ 458 474
- Tchekhovskoy, A., Narayan, R. and McKinney, J. 2011, MNRAS Letters 418 79
- Tchekhovskoy, A., McKinney, J. 2012, MNRAS Letters 423 55
- Telfer, R., Zheng, W., Kriss, G., Davidsen, A. 2002, ApJ 565 773 **T02**
- Threlfall, J. et al 2012, A & A 544 24
- Yamada, M. 2007, Physics of Plasmas 14 058102
- Zheng, W. et al. 1997, ApJ 475 469
- Zhu, Y. et al. 2012, MNRAS 424 2504
- Willott, C., Rawlings, S., Blundell, K., Lacy, M. 1999, MNRAS 309 1017